



**HAL**  
open science

# Black Holes and Galactic Density Cusps I Radial Orbit Cusps and Bulges

Richard Henriksen, Morgan Le Delliou, Joseph D. Macmillan

► **To cite this version:**

Richard Henriksen, Morgan Le Delliou, Joseph D. Macmillan. Black Holes and Galactic Density Cusps I Radial Orbit Cusps and Bulges. 2009. hal-00431275v1

**HAL Id: hal-00431275**

**<https://hal.science/hal-00431275v1>**

Preprint submitted on 11 Nov 2009 (v1), last revised 20 Mar 2011 (v7)

**HAL** is a multi-disciplinary open access archive for the deposit and dissemination of scientific research documents, whether they are published or not. The documents may come from teaching and research institutions in France or abroad, or from public or private research centers.

L'archive ouverte pluridisciplinaire **HAL**, est destinée au dépôt et à la diffusion de documents scientifiques de niveau recherche, publiés ou non, émanant des établissements d'enseignement et de recherche français ou étrangers, des laboratoires publics ou privés.

# Black Holes and Galactic Density Cusps I

## Radial Orbit Cusps and Bulges

R.N. Henriksen<sup>1</sup>, M. Le Delliou<sup>2</sup>, and J.D. MacMillan<sup>3</sup>

<sup>1</sup> Queen's University, Kingston, Ontario, Canada  
e-mail: henriksn@astro.queensu.ca

<sup>2</sup> Instituto de Física Teórica UAM/CSIC, Facultad de Ciencias, C-XI, Universidad Autónoma de Madrid  
Cantoblanco, 28049 Madrid SPAIN  
e-mail: Morgan.LeDelliou@uam.es

<sup>3</sup> Faculty of Science, University of Ontario Institute of Technology, Oshawa, Ontario, Canada L1H 7K4  
e-mail: joseph.macmillan@gmail.com

### Abstract

*Aims.* In this paper we study density cusps made from radial orbits that may contain central black holes. The actual co-eval self-similar growth would not distinguish between the central object and the surroundings.

*Methods.* To study the environment of an existing black hole we seek distribution functions that may contain a black hole and that retain at least a memory of self-similarity. We refer to the environment in brief as the 'bulge' or sometimes the 'halo'. This depends on whether the black hole is a true singularity dominating its halo or rather a core mass concentration that dominates a larger bulge. The hierarchy might extend to include galactic bulge and halo.

*Results.* We find simple descriptions of simulated collisionless matter in the process of examining the presence of central masses. The Fridmann & Polyachenko distribution function describes co-eval growth of a bulge and black hole that might explain the observed mass correlation.

*Conclusions.* We derive our results from first principles assuming either self-similar virialisation or normal steady virialisation. The implied energy relaxation of the collisionless matter is due to the time dependence. Phase mixing relaxation may be enhanced by clump-clump interactions.

**Key words.** theory-dark matter-galaxies:haloes-galaxies:nuclei-black hole physics-gravitation.

## 1. Introduction

The relation between the formation of black holes and of galaxies has developed into a key astrophysical question. From the early papers by Kormendy and Richstone (KR1995), to the more recent discoveries by Magorrian et al. (Ma98), Ferrarese and Merritt (Ferrase & Merritt 2000), and Gebhardt et al. (Gebhardt et al., 2000). These papers establish a strong correlation between what is essentially the black hole mass and the surrounding stellar bulge mass (or velocity dispersion). The origin of this proportionality, which extends well beyond the gravitational dominance of the black hole, remains unproven. But it is generally taken to imply a coeval growth of the black hole and bulge.

We know that much of the black hole growth into super massive black holes takes place in a dissipative fashion involving baryons during the AGN (Active Galactic Nuclei) phase. In this phase the accretion rate (and therefore the black hole mass given a cosmological time scale) is limited by either a Bondi type choke point or by the Eddington radiation limit. The mass source is either diffuse gas or tidally disrupted stars. The observed AGN luminosities are in rough agreement with the mass accretion rates that are necessary to grow the super massive black holes, assuming substantial black hole 'seeds' initially.

The tidal disruption of an individual star causes sporadic flaring of the AGN. One expects the mean accretion rate

of this sort to be set by slow diffusion from an essentially collisionless stellar environment (e.g. Bahcall & Wolf 1976, Merritt & Szell 2006) into the 'loss cone'. This is thought to end in a steady zero flux limit (Bahcall & Wolf 1976) with a density cusp proportional to  $r^{-7/4}$ . However this process is generally slow, requiring at least a relaxation time (e.g. Merritt & Szell 2006).

Various proposals have been offered to explain the black hole mass-bulge mass proportionality as a consequence of the AGN phase. There is as yet no generally accepted scenario although a kind of 'auto-levitation' or feed-back mechanism is plausible. In any event there remains the question of the origin of the seed masses. In some galaxies at very high red shift the inferred black hole masses are already of order  $10^9 M_{\odot}$  (e.g. Kurk et al., 2007) after about one Ga of cosmic time. This may require frequent, extremely luminous early events (e.g. Walter et al., 2009), or it may suggest an alternate growth mechanism.

The latter possibility is reinforced by the detection of a change in the normalization of the black hole mass-bulge mass proportionality in the sense of relatively larger black holes at high red shift (e.g. Maiolino et al. 2007). As suggested in that paper it seems that the black holes may grow first, independently of the bulge.

Recently (Peirani & de Freitas Pacheco 2008) have studied the possible size of the dark matter component in black hole masses. By assuming that the 'pseudo phase space density' (e.g. H2006) is strictly constant they convert the relativistic accretion

of the dark matter into an adiabatic Bondi flow problem and obtain the resulting accretion rate. Then by adopting the mass proportionality above and fitting boundary conditions from cosmological halo simulations, they deduce that between 1% and 10% of the black hole mass could be due to dark matter.

The pseudo-density assumption may be questionable, but if we accept this result at face value, it seems that a seed mass of say  $10^6 M_\odot$  could have grown from dark matter. It would now be part of a super massive black hole that subsequently grew in the AGN phase. Some seeds may be primordial. As early as 1978 fully relativistic collapse calculations (Bicknell & Henriksen 1979) predicted primordial black hole masses in the range  $10^2$  to  $10^6 M_\odot$ .

Density cusps surrounding black holes have been studied extensively. Classic studies by (Peebles 1972) and by (Bahcall & Wolf 1976) dealt with the problem of feeding the black hole. In addition to these diffusion studies, Young (Young 1980) explored the cusps produced by the adiabatic growth of a black hole in a pre-existing isothermal stellar environment. This was extended by (Quinlan et al 1995) and by (MacMillan & Henriksen 2002) to more general environments. The conclusions were that the black hole induced cusps were never flatter than  $r^{-1.5}$  (the isothermal case) and that no black hole mass-bulge mass correlation was established (MacMillan & Henriksen 2002). This latter conclusion has spurred the investigation of coeval dynamical growth of the black hole and bulge in contrast to adiabatic growth (MacMillan & Henriksen 2003).

Such concerns have passed from the abstract to the practical with the detection of stellar cusps around galactic nuclear black holes (Gillessen et al., 2009). This latter paper reports stellar cusp power laws for the central Milky Way in the range  $-1.1 \pm 0.3$ , significantly shallower than the adiabatic  $-1.5$  or the zero flux  $-1.75$ . We seek to find under what general conditions such power laws may arise in this series of papers. We note also that the measured stellar orbits for the Milky Way cusp (Gillessen et al., 2009) show them to be mainly isotropic, although some may be found in an outer disc or discs.

An effective method of evolving flat cusps is to invoke tight binary black hole systems produced by mergers that 'scour' the stellar environment (e.g. Merritt & Szell 2006, Nakano & Makino 1999). Depending on the power law assumed for the initial stellar environment, Merritt and Szell simulate scoured power laws that can be as flat as  $-1$  in an initially  $-1.5$  cusp, and as flat as  $-0.5$  in an initially  $-1$  stellar cusp. Flatter values are reduced to essentially constant density cores. The  $-1$  slope as noted above is a reasonable fit to the Milky Way (ibid).

Subsequently, but taking at least the central relaxation time, the cusps should regenerate to the zero flux condition ( $r^{-1.75}$ ) according to the simulations in (Merritt & Szell 2006). However this will extend only out to about 0.2 of the gravitational influence radius of the black hole. This regeneration is not thought to be relevant to the Milky Way central stellar cusp, but may be present on small scales elsewhere.

Such a picture is seductive, especially given the recent detection of a strong correlation between the nuclear black hole mass and the central luminosity deficit (Kormendy & Bender 2009). However the correlation in itself only implicates the influence of the black hole. It does not necessarily require the merger history, which in any case is unlikely to be the same for different galaxies. Consequently we explore in this series of papers (I, II, III) whether cusps as flat as those resulting from scouring might also be produced during the dynamical formation of the black hole. In this first paper we present a summary of the situation for ra-

dial orbits since the arguments are typical but easily carried out in that case. The results may apply to the outer (beyond the NFW scale radius) regions of dark matter halos.

Our technique will be to infer reasonable distribution functions for collisionless matter from the time dependent Vlasov and Poisson set, augmented by an initially dominant central mass. For consistency we will study cases where the loss cones are not empty, since we are investigating dynamical evolution of the system. This temporal evolution allows for relaxation of collisionless matter in addition to possible 'clump-clump' (two clump) interactions.

We adopt a system of coordinates that allows us either to readily take the self-similar limit or to retain a memory of previous self-similar dynamical relaxation. In this way we can remain 'close' to self-similarity just as the simulations appear to do. These coordinates (H2006, H2006A) allow the general expression of the Vlasov-Poisson set, but they also contain the parameter that reflects underlying self-similarity. The self-similar limit is taken by assuming 'self-similar virialisation', wherein the system is steady in these coordinates although not absolutely steady since mass is accumulating.

We begin the next section with the general formulation in spherical symmetry. Subsequently we discuss the various possible distribution functions (DF from now on) for radial orbits. Finally we show that the DF of Fridmann and Polyachenko (hereafter FPDF, Fridmann & Polyachenko 1984) can be generated through the technique of coarse graining (HLeD 2002) and then give our conclusions.

## 2. Dynamical Equations in Infall Variables

Following the formulation of H2006 we transform to infall variables the collisionless Boltzmann and Poisson equations for a spherically symmetric anisotropic system in the 'Fujiwara' form (e.g. Fujiwara 1983) namely

$$\frac{\partial f}{\partial t} + v_r \frac{\partial f}{\partial r} + \left( \frac{j^2}{r^3} - \frac{\partial \Phi}{\partial r} \right) \frac{\partial f}{\partial v_r} = 0, \quad (1)$$

$$\frac{\partial}{\partial r} \left( r^2 \frac{\partial \Phi}{\partial r} \right) = 4\pi^2 G \int f(r, v_r, j^2) dv_r dj^2, \quad (2)$$

where  $f$  is the phase-space mass density,  $\Phi$  is the 'mean' field gravitational potential,  $j^2$  is the square of the specific angular momentum and other notation is more or less standard.

The transformation to infall variables has the form (e.g. H2006)

$$\begin{aligned} R &= r e^{-\alpha T / a}, & Y &= v_r e^{-(1/a-1)\alpha T}, \\ Z &= j^2 e^{-(4/a-2)\alpha T}, & e^{\alpha T} &= \alpha t, \\ P(R, Y, Z; T) &= e^{(3/a-1)\alpha T} \pi f(r, v_r, j^2; t), & (3) \\ \Psi(R; T) &= e^{-2(1/a-1)\alpha T} \Phi(r), & \Theta(R; T) &= \rho(r, t) e^{-2\alpha T}. \end{aligned}$$

The passage to the self-similar limit requires taking  $\partial_T = 0$  when acting on the transformed variables. Thus the self-similar limit is a stationary system in these variables, which is a state that we refer to as 'self-similar virialisation' (HW 1999, Le Delliou 2001). The virial ratio  $2K/|W|$  is a constant in this state (although greater than one;  $K$  is kinetic energy and  $W$  is potential), but the system is not steady in physical variables as infall continues.

The single quantity  $a$  is the constant that determines the dynamical similarity, called the self-similar index. It is composed of two separate reciprocal scalings,  $\alpha$  in time and  $\delta$  in space, in the form  $a \equiv \alpha/\delta$ . As it varies it contains all dominant physical constants of mass, length and time dimensions, since the mass scaling  $\mu$  has been reduced to  $3\delta - 2\alpha$  in order to maintain Newton's constant  $G$  invariant (e.g. H2006).

We assume that time, radius, velocity and density are measured in fiducial units  $r_o/v_o, r_o, v_o$  and  $\rho_o$  respectively. The unit of the distribution function is  $f_o$  and that of the potential is  $v_o^2$ . We remove constants from the transformed equations by taking

$$f_o = \rho_o/v_o^3, \quad v_o^2 = 4\pi G\rho_o r_o^2. \quad (4)$$

These transformations convert equations (1),(2) to the respective forms

$$\begin{aligned} & \frac{1}{\alpha} \partial_T P - (3/a - 1)P + \left(\frac{Y}{\alpha} - \frac{R}{a}\right) \partial_R P \\ & - \left( (1/a - 1)Y + \frac{1}{\alpha} \left( \frac{\partial \Psi}{\partial R} - \frac{Z}{R^3} \right) \right) \partial_Y P - (4/a - 2)Z \partial_Z P = 0 \end{aligned} \quad (5)$$

and

$$\frac{1}{R^2} \frac{d}{dR} \left( R^2 \frac{\partial \Psi}{\partial R} \right) = \Theta. \quad (6)$$

This integro-differential system is closed by

$$\Theta = \frac{1}{R^2} \int P dY dZ. \quad (7)$$

We consider in this paper the filled loss cone limit of radial infall (HLeD 2002). This is mainly as a test of our techniques although it may have application on large scales. To proceed we set  $P = F(R, Y; T) \delta(Z)$  ( $\delta(\cdot)$  is the Dirac delta, not the scaling delta) which changes the scaling for the DF to

$$\pi f = F(R, Y, ; T) e^{(1/a-1)\alpha T} \delta(j^2), \quad (8)$$

while other scalings remain unchanged.

The governing equations now become (6) plus

$$\begin{aligned} & \frac{1}{\alpha} \partial_T F + (1/a - 1)F + \left(\frac{Y}{\alpha} - \frac{R}{a}\right) \partial_R F \\ & - \left( (1/a - 1)Y + \frac{1}{\alpha} \frac{\partial \Psi}{\partial R} \right) \partial_Y F = 0. \end{aligned} \quad (9)$$

Finally equation (7) reduces to

$$\Theta = \frac{1}{R^2} \int F dY. \quad (10)$$

This completes the formalism that we will use to obtain the results below. We begin in the next section with the radial limit. The 'cusps' we describe there will generally end in what is the central 'bulge' surrounding the black hole, rather than in the black hole itself.

### 3. Radial Orbit Steady Cusps and Bulges

We expect one mode of relaxation in collisionless cusps to be of the 'moderately violent' type satisfying, in terms of the particle energy  $E$  and mean field potential  $\Phi$ , the relation

$$\frac{dE}{dt} = \frac{\partial \Phi}{\partial t} \Big|_r. \quad (11)$$

This includes phase-mixing. Another mode (Diemand et al., 2006) is furnished by the presence of hierarchical sub-structure. The sub-structure can interact in clump-clump interactions that can induce relaxation on a coarse-grained scale (H2009).

However the temporal evolution of the system is difficult to follow analytically even in the self-similar limit, so we normally look for equilibria established by the evolution. This may be either a strictly steady state in some appropriate coarse-grained description, or it may be a self-similar virialised state. The memory of the temporal relaxation is incorporated into the parameter  $a$  as indicated above.

One can allow for the presence of a black hole by iterating about an equilibrium state determined initially by the black hole. This allows the central mass and the environment to evolve together towards a new equilibrium, although normally only a single loop is feasible.

Using the characteristics of equation (9) plus

$$\frac{d\Psi}{ds} = \frac{\partial \Psi}{\partial s} + \frac{dR}{ds} \partial_R \Psi \quad (12)$$

where  $ds \equiv \alpha dT$ , one finds by a simple manipulation that

$$\frac{d\left(\frac{Y^2}{2} + \Psi\right)}{ds} = -2(1/a - 1) \frac{Y^2}{2} - \frac{R}{a} \partial_R \Psi + \frac{\partial \Psi}{\partial s}. \quad (13)$$

In order for this equation to yield the energy as an isolating integral (i.e. characteristic constant) the last two terms must sum to give  $-2(1/a - 1)\Psi$ . This is most simply effected by setting  $\partial \Psi / \partial s = 0$  and  $R \partial_R \Psi = p\Psi$ , which turns out to be a condition for both self-similarity and a steady state,<sup>1</sup> where

$$p = 2(1 - a). \quad (14)$$

Whence, setting  $\mathcal{E} \equiv Y^2/2 + \Psi$ , we have

$$\frac{d\mathcal{E}}{ds} = -2(1/a - 1)\mathcal{E}. \quad (15)$$

This variation does render  $E$  constant on characteristics (and therefore in time) as one sees by integrating to the form  $E_o \exp(-2(1/a - 1)s)$ , and then by using the transformations (3) to find  $E = \mathcal{E} \exp(2(1/a - 1)\alpha T) \equiv E_o$ . Such a state occurs for example in a system whose potential is dominated by the central mass, for which  $a = 3/2$  and  $p = -1$ .

Equation (9) also yields along the characteristic

$$\frac{dF}{ds} = -(1/a - 1)F, \quad (16)$$

so that with equation (15)

$$F = \tilde{F}(\kappa) |\mathcal{E}|^{1/2}. \quad (17)$$

<sup>1</sup> The general solution to the sum condition is  $\Psi = R^p G(r)$  where the function  $G(r)$  is arbitrary: however this leads only to the general Jeans form.

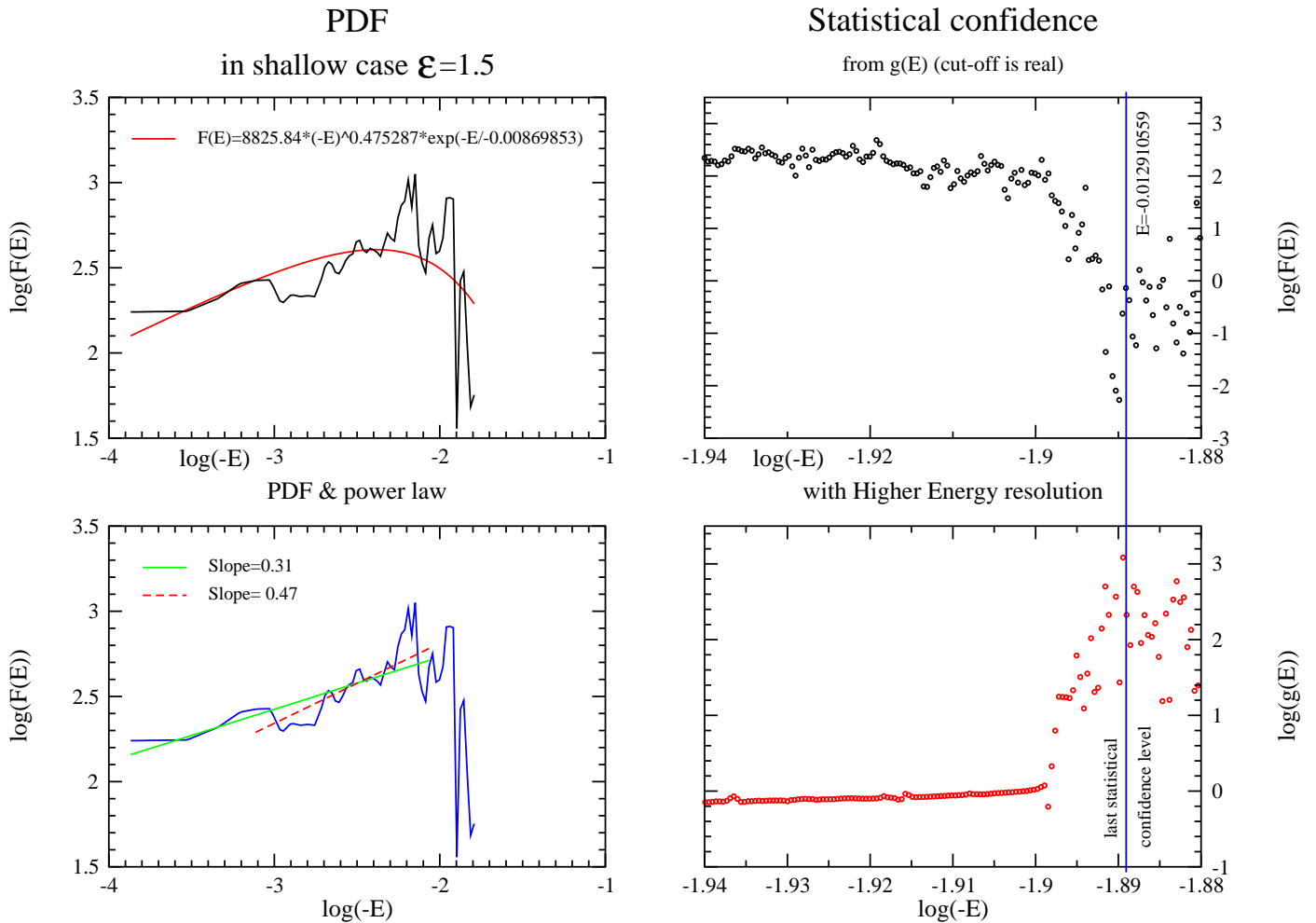


**Figure 1.** A shell code evaluation of the DF (Le Delliou 2001), evolved from a system with initial density  $\rho \propto r^{-1.5}$ . The first fit is with a cut off power law ( $F \propto E^{-p} e^{-E/E_c}$  with  $p \simeq 1/2$ ,  $E_c \simeq -10^{-2}$ ; upper left panel), while the second fit is just a power law (lower left), confirming HW 1999. The cut off is confirmed by higher resolution in the DF (upper right) and in density of states  $g(E)$  (lower right).

The steady unscaled DF follows from this last equation and the transformations (3) as ( $a \neq 1$ )

$$\pi f = \tilde{F}(\kappa) |E|^{1/2} \delta(j^2). \quad (18)$$

An upper energy cut-off  $E_+ \propto \Phi$  is required for finiteness in the positive energy ( $a < 1$ ) case. In general one can add an arbitrary constant  $E_o$  to  $E$  in this expression, which reflects the constant in the potential. A large positive constant would express a negative energy cut-off at the value  $-E_o$  and the DF would increase toward zero energy.

The quantity  $\kappa$  in equation (18) labels any other possible characteristic constant, but in general nothing is readily available. One does find additional constants with coarse graining as is discussed below.

The DF (18) with  $\tilde{F}$  constant describes a steady system of radial orbits at the end of self-similar evolution characterized by the index  $a$ . It was found previously (HW95), and in (HW 1999)

it was shown to be a natural end state for self-similar infall. The potential and density laws take the form<sup>2</sup> ( $a \neq 1$ )

$$\Psi = \Psi_o R^{(2-2a)}, \quad \Theta = 2(3-2a)(1-a)\Psi_o R^{-2a}. \quad (19)$$

In the context of a dominant central ‘black hole’, we can use this DF to generate a ‘near Keplerian’ system by taking  $a = 3/2$ . This yields a point mass potential surrounded by massless particles. The massless particles may be distributed in any manner, but self-similarity suggests that the number density  $N$  should vary as  $N \propto e^{-3s/a} R^{-3} \propto r^{-3}$ . Such a halo could exist outside any dominant mass as was discussed in (HW 1999).

The direct density integral over the DF (18) yields for  $\rho$

$$\rho = \frac{\pi \tilde{F}}{\sqrt{2}} \frac{|\Phi|}{r^2}. \quad (20)$$

Hence one can include a central mass by iteration, beginning with a point mass potential for  $\Phi$  in the density (20), and then

<sup>2</sup> We have used our current notation when using the results of previous papers, in which  $\delta, X, S$  in (HW 1999) are respectively  $1/a, R, \Theta R^2$ . In (HW95)  $\delta$  there becomes  $1/(1-a)$  in current notation.

using the Poisson equation to obtain a new potential in a form that is no longer self-similar. This yields

$$\Phi = -\frac{M_* + C_2(1 + \ln r)}{r}, \quad (21)$$

whence follows a new density by (20). The constant  $M_*$  would be the central mass while  $C_2 = \pi\tilde{F}/\sqrt{2}M_*$ . There is only a logarithmic modification to the  $r^{-3}$  law at large  $r$ , but at small  $r$  the density flattens. Since this is only the first iteration cycle, the expression is unlikely to apply very near the central mass where formally it declines to zero. The large scale behaviour does not fit the bulge simulations inside the NFW (NFW) scale length, but it could describe the halo region outside a central bulge of mass  $M_*$ .

Since the density is linear in the potential we may solve for a self-consistent cusp having the DF (18) by letting the potential be determined by the Poisson equation. Working in transformed variables we find

$$\Psi = -AR^{p_-} - BR^{p_+}, \quad (22)$$

where  $A, B$  are arbitrary real constants  $> 0$  and

$$p_{\pm} = -\frac{1}{2} \pm \sqrt{\frac{1}{4} - \frac{\pi}{\sqrt{2}}\tilde{F}}. \quad (23)$$

By letting  $\tilde{F} \rightarrow 0$  we see that  $p_-$  is the power that should be taken near the centre if we wish to create a strong central mass concentration. It tends to  $-1$  in this limit while  $p_+$  tends to zero. Hence we set  $B = 0$  in this limiting domain. The potential then satisfies our basic condition (14) with a new self-similar index. This is given by  $a = 1 - p_-/2$  or explicitly

$$a_- = \frac{5}{4} + \frac{1}{2} \sqrt{\frac{1}{4} - \frac{\pi}{\sqrt{2}}\tilde{F}}. \quad (24)$$

Equation (19) now gives the inner cusp density law as

$$\Theta = |p_-|(1 + p_-)|\Psi_o|R^{(-2+p_-)}. \quad (25)$$

This can not be flatter than  $R^{-2.5}$ , which appears only for the ‘maximum bulge’ for which  $\tilde{F} = 1/(2\pi\sqrt{2})$ .

In the context of dark matter simulations such a steady halo of radial orbits could describe the region just beyond the NFW scale radius, based on the density profile alone. It is not stable in a strict steady state according to the usual Antonov criteria (e.g. Binney & Tremaine 1987), unless the energy is negative. Consequently we do not expect it in central regions where  $a < 1$  where the energy is positive (with a central zero: the potential increases outward according to Eq. 19). The radial velocity dispersion is  $\overline{v_r^2} = |\Phi|/2$ . In paper II we shall see that although this DF is not unique, alternate DF’s are biased towards zero angular momentum.

In (HW 1999) weak evidence was presented to show that the  $|E|^{1/2}$  law did appear near the end of the infall for the most tightly bound particles. This was re-enforced by additional Lagrangian shell code evolution from Le Delliou 2001 (see figure 1). We have therefore considered its implications at length here. However the DF (18) does *not* appear in high resolution simulations of radial orbit *growing* isolated halos (e.g. MacMillan 2006) in a state of self-similar virialisation (HW 1999). In such a state, infall continues. Instead of the steady DF, the DF of Fridmann and Polyachenko (hereafter

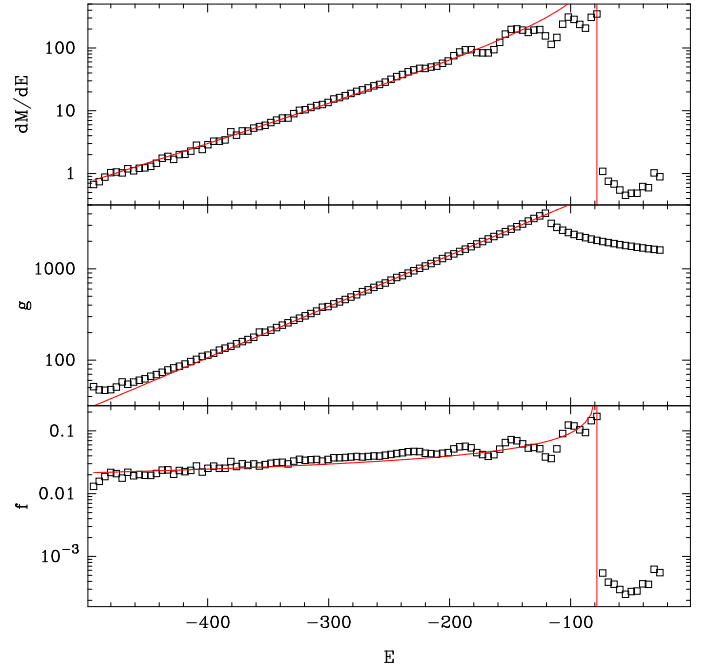


**Figure 2.** We show the Fridmann and Polyachenko fit to the mass distribution  $dM/dE = f(E).g(E)$ , density of states  $g(E)$ , and the phase space distribution function  $f(E)$ . The figure is based on the radial simulations of an isolated dark matter halo by MacMillan (MacMillan 2006). The system is maintained in self-similar virialisation by steady accretion. The fits use equation (26) with  $K = -E_o/(4\sqrt{2}\pi^3)$  and  $E_o \approx -80$  in machine units.

FPDF, Fridmann & Polyachenko 1984) is found to predict accurately all of the measured quantities as in the accompanying figures. These include an inverse square density law and a power law pseudo phase space density of  $\approx -1.5$  (MacMillan 2006; there are logarithmic corrections to the power law). The latter power is flatter (MWH 2006) than is generally found in full cosmological simulations. These results are illustrated in figures (2) and (3).

This DF (Fridmann & Polyachenko 1984) used to make the fits in figures (2) and (3) is

$$f = \frac{K}{(-E + E_o)^{1/2}} \delta(j^2), \quad (26)$$

for  $E < E_o \leq 0$ , and  $r \leq r_f$  (where  $\Phi(r_f) = E_o$ ) and zero otherwise. In an infinite system we may take  $E_o = 0$ . The density profile is  $r^{-2}$  and the potential is logarithmic. The logarithmic variation of the velocity dispersion together with the inverse square density profile accounts for the pseudo density approximate power law found in the simulations (MacMillan 2006).

By using our method of coarse graining, we show below that the effective index  $a = 1$  in this mode (hence the measured potential is indeed logarithmic as follows with coarse graining when  $a = 1$ ). Thus the deduction above of the DF (18) does not apply (nor do the arguments of HW95 where  $a = 1$  was inadvertently excluded). The limit of  $a = 1$  always needs to be discussed separately.

The rather precise fit of a pure function of the energy to the DF of a time dependent non-closed system (MacMillan 2006) is somewhat surprising. We expect that  $E = E(t)$  so that it is no longer an isolating integral and (with  $K$  constant) the DF (26) is no longer strictly a solution of the Boltzmann equation.

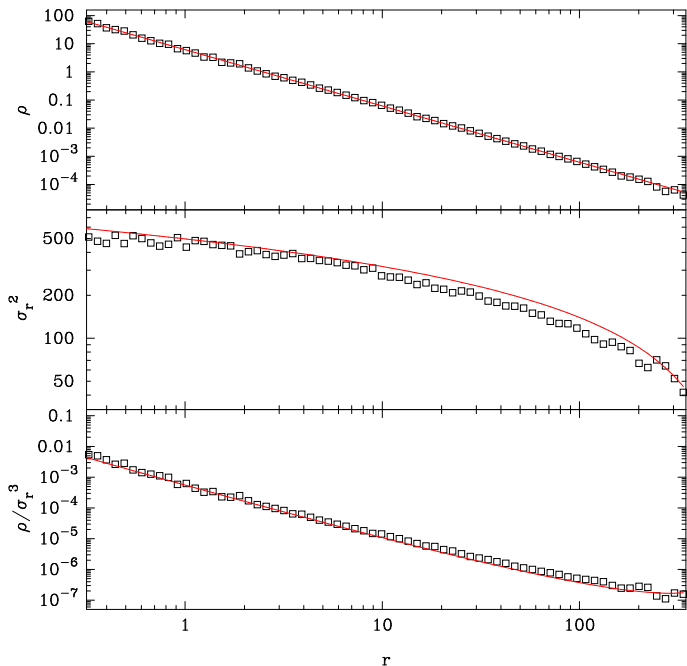


**Figure 3.** We show the the Fridmann and Polyachenko fit to the mass density, the velocity dispersion and the ‘pseudo phase space density’ for the same simulations by MacMillan.

However if we assume the separated form  $f = K(t)F(E)\delta(j^2)$  then  $d \ln K / dt + d \ln F / dE \partial_t \Phi = 0$  from equation (5). With  $F(E)$  as in equation (26) we obtain  $d \ln F / dE = 1 / (2(-E + E_o))$ . Thus with  $|E|$  sufficiently large or  $\partial_t \Phi$  sufficiently small,  $K$  is approximately constant.

The persistence of this DF is also undoubtedly due to the strict proscription of non-radial forces in the simulations. It is not linearly stable by the Antonov criteria for  $E < 0$ . When this proscription is relaxed (MacMillan 2006) shows that the equilibrium Fridmann and Polyachenko DF is subject to the radial orbit instability. It may require continual non-equilibrium excitation as provided by steady infall to be realized.

The unique feature of the distribution function (26) is that the density is independent of the potential. Hence one can simply add a point mass potential to the logarithmic bulge value and the density will remain  $\sqrt{2\pi}Kr^{-2}$ . The velocity dispersion however goes as  $\overline{v_r^2} = |\Phi - E_o|$  and we may take  $\Phi = -M_*/r + \sqrt{2\pi}K \ln r + E_o$ . Normally the log term is negative since  $r \leq r_f$ , and here  $r_f = r_o$ . MacMillan (ibid) finds a good fit to this radial dispersion in his simulations without a central mass.

In the next section we seek the origin of the FPDF from self-similarity by using a coarse-graining expansion, first discussed in (HLeD 2002). We seek the origin of the Fridmann and Polyachenko DF. This approach has been used extensively since the original paper in such works as (H2006, H2007 and H2009). The simplest procedure which terminates the series at first order and so produces constraints on the maximally coarse-grained, steady, DF remains useful. We outline the procedure in the next section, but the principal result is that the Fridmann and Polyachenko distribution function can be understood as a self-similar DF with  $a = 1$  in addition to equation (18). We do this by finding that only these two distribution functions are independent of initial conditions.

#### 4. Coarse-Grained Radial Distribution Functions

We follow the procedure introduced in (HLeD 2002) wherein we write

$$F = F_o + \frac{F_1}{\alpha} + \frac{F_2}{\alpha^2} + \dots \quad (27)$$

and allow  $\alpha$  to become large while holding the similarity index  $a$  constant. Substituting this expansion into equation (9) while insisting on self-similarity ( $\partial_r = 0$ ) and solving by the method of characteristics yields

$$F_o = F_{oo}(\zeta, r)R^{(1-a)}. \quad (28)$$

The characteristic constants are

$$\zeta \equiv \frac{Y}{R^{(1-a)}}, \quad (29)$$

$$r \equiv Re^{s/a},$$

and  $s$  is measured along a characteristic. The radius  $r$  may be taken as the initial position of a particle on the characteristic. We have usually regarded the characteristics as geometrical objects (here  $s$  is independent of  $T$ ) and we have taken  $r = 1$  so that  $s = 0$  is at the same radius on each characteristic. This is correct in a statistical sense once the system is well developed in self-similar virialisation, but it does not allow us to retain the memory of an initial distribution of particles, which a dependence on a variable  $r$  implies.

Generally we ignore any dependence on initial conditions except as they are contained in  $a$ , since otherwise it leads to

$$I_{oo} \equiv \int F_{oo} d\zeta, \quad (30)$$

being a function of  $r$ , which prevents a term by term solution for the potential. However we will retain this dependence on  $r$  in  $F_{oo}$  temporarily, even while continuing to assume that  $I_{oo}$  is independent of  $r$ . It is the eventual reconciliation of these assumptions that leads to (26).

We observe that, although in the final DF,  $r$  from equations (3) may be considered identical with that in equation (29), they should be kept separate during the characteristic analysis. The radius in equation (3) is general while that in equation (29) is constant on a characteristic.

Proceeding to the first order term following the procedure in (HLeD 2002) we obtain that  $F_1 = 0$  (giving  $F_o$  as correct to order  $1/\alpha^2$ ) is possible provided that  $F_{oo}$  satisfies

$$\partial_\zeta F_{oo} \left( (1-a)\zeta^2 + \frac{I_{oo}}{3-2a} + \frac{\gamma_\star}{R^{(3-2a)}} \right) - \zeta r \partial_r F_{oo} - (1-a)\zeta F_{oo} = 0. \quad (31)$$

We have set  $\Psi_\star = -(M_\star/r)e^{-2(1/a-1)\alpha T} = -\gamma_\star/R$ , where  $M_\star$  is a central point mass. Thus  $M_\star = \gamma_\star e^{(3/a-2)\alpha T}$ , and so the central mass grows self-similarly (HW 1999) if  $\gamma_\star$  is constant. A solution of equation (31) is easily found by characteristics. Suffice it to say for brevity that, for general  $a$ , the only solution consistent with our assumption of self-similar virialisation and  $I_{oo}$  independent of  $r$  requires  $M_\star = 0$ . Consequently one finds  $F_o = K|E|^{1/2}(R/r)^{(1-a)}$  so that  $\pi f_o = K|E|^{1/2}\delta(j^2)$ , just as reported above.

However the special case  $a = 1$  is more interesting. The characteristics of equation (31) show (note that  $\gamma_\star/R = M_\star/r$ ) that

$F_{oo} = F_{oo}(E)$ , where the energy can be taken as (restoring units)

$$E = \frac{v_r^2}{2} + I_{oo} \ln r - \frac{GM_*}{r}. \quad (32)$$

The strong  $r$  dependence in the potential, and hence in  $E$ , implies that only the Fridmann-Polyachenko solution is consistent with  $I_{oo}$  being independent of  $r$ , as was assumed initially. This is because the distribution function (26) yields an integral for  $I_{oo}$  (30) that is independent of the potential, and hence of the initial conditions. We expect this to be the fully relaxed state. The density to this order is  $\rho_o = I_{oo}/r^2 = \int \pi f d v_r$  using (26) where we write the result in terms of the coarse graining constant. The DF (18) appears when the independence of  $r$  is assumed consistently in the coarse graining, and when as above a strict steady state is enforced.

This is the only way in which the Fridman and Polyachenko DF appears naturally as a description of self-similar virialisation using our methods. It is self-similar but not exactly steady. Proceeding farther in the series (27), either by terminating at second order or by renormalising, will give small corrections to this result (H2006, H2007) that describe the approach to equilibrium. This DF remains our best description of interrupted radial accretion onto a central point mass.

## 5. Completely Relaxed, Nearly Inverse Square, Solution

A careful treatment of the  $a = 1$  radial, exactly steady state, in the fashion of (HW95) (not given there, although the relevant equations are given and may be translated into our notation and solved) yields a logarithmic potential and an inverse square density law to within logarithmic corrections. We use the formulation of (HW95). The DF takes the Gaussian form

$$F = K e^{(-2E/\Psi_o)} \delta(v_\theta) \delta(v_\phi), \quad (33)$$

where  $E \equiv v_r^2/2 + \Psi_o \ln(\delta r)$  in terms of the kinetic and potential energies. This reveals the solution as the singular isothermal sphere ( $\rho \propto r^{-2}$ ) with only radial orbits present.

We require  $\Psi_o > 0$  in order to have an attractive gravitational force. In a negative energy region  $E$  might be replaced by  $E_o - E$  where  $\Phi \leq E \leq E_o < 0$  to allow for an arbitrary reference potential. In the presence of a dominant central point mass the energy will be negative and  $\Psi_o$  should be replaced by the total potential  $|\Phi|$ .

The solution is only valid to logarithmic accuracy however since, although a logarithmic potential corresponds exactly to an inverse square density law, the density integral over the DF (33) gives

$$\rho = \frac{\sqrt{\pi} \operatorname{erf}(2) K}{r^2} |\Phi|^{1/2}. \quad (34)$$

This gives a logarithmic correction to the density from the potential, so the solution is not in fact self-similar. An iteration by using this density in the Poisson equation is now possible. At least this is true near the black hole where the point mass potential dominates. However the iteration does not converge rapidly.

## 6. Discussion

The growth rate of a central mass (i.e. a collisionless concentration, not a true black hole) from a reservoir of radial orbits is zero if there is a true steady state. However in a state of self-similar

virialisation we can expect them to settle into a bulge as they become trapped by the increasing mass. The growth rate is not zero if the central mass is a black hole, since then the outward bound radial orbits are suppressed. In that case however the steady state is only a crude approximation, and the true timescale would be the free-fall time of the bulk of the accreting mass. It is unlikely that a black hole can grow directly from a large scale system of radial orbits since there is no reason why the distant particles should ‘know’ where it is.

The radial alignment required to hit a growing black hole from a few hundred parsecs is at least one part in  $10^8$  to  $10^{10}$  depending on its mass! This suggests that instead (see e.g. MacMillan & Henriksen 2003) the actual growth is by way of a multi-stage process. In the first stage, radial orbits accrete from the galactic halo to form a bound spherical bulge of intermediate size, due to finite angular momentum about the centre. They are trapped there either by the usual mechanism of self-similar infall as the potential increases in time with increasing internal mass, or by dissipative interactions. If there is substructure in the collisionless matter (e.g. stars and dark matter clumps), then these are able to produce dissipational collisions. Ultimately these collisions and tidal interactions can lead to a more gradual growth of a more central mass (e.g. MacMillan & Henriksen 2003 in the Carnegie meeting).

Moreover the radial orbit instability can lead to the development of a bar (MWH 2006). This bar can then transport angular momentum away from the bulge by the ejection of particles. Such ‘interrupted accretion’ may repeat several times on the way to the actual central object. The rapid radial accretion of a bulge is in fact the way in which dark matter halos are thought to grow (Zhao et al., 2003, Lu et al. 2006) initially. This is then followed by a slower growth phase. The DF (26) can be used to describe the environment of the central mass on each scale of the interrupted cascade.

In the previous section we have discussed distribution functions that have been found to describe simulated radial collisionless systems. Only the steady DF (18) allows for a memory of the preceding dynamics, but a black hole can only be included in the system by iteration. The radial orbit singular isothermal sphere DF (33) gives an approximate  $r^{-2}$  density cusp, but a central black hole is not easily treatable.

The most successful DF that persists during infall and that contains a central point mass is that of Fridmann and Polyachenko (26). This yields an inverse square density cusp and a velocity dispersion that first decreases and then increases with radius. It may apply in the shells of ‘interrupted accretion’ discussed above.

In this connection we refer to the work of Mutka (Mutka 2009) on gravitationally lensed galaxies with double images. He concludes that there are two classes of density cusps with the larger sample (about 80%) showing a logarithmic density slope of  $\approx -1.95$  well inside the NFW scale radius. The other 20% show this slope as  $\approx -1.45$ . These may be unresolved triple image lens and, if so, the measured value should be rejected.

Mutka’s result is a measure of the total mass distribution rather than just the dark matter. Perhaps we are seeing enhanced relaxation in the mixture of stars and dark matter, that leads towards an isothermal cusp, rather than the shallower cusps of the dark matter simulations. It is significant that this inverse square slope is also frequently found by direct dynamical modelling of galaxies (van der Marel 2009).

However an inverse square slope is not restricted to a system of purely radial orbits as the isotropic isothermal distribution



shows. In the next paper we survey anisotropic distribution functions in spherical spatial symmetry that also have a self-similar memory. Some of these also provide an inverse square density profile.

The significance of the hierarchy of co-evolving structures is that there will always be a mass correlation between them. Thus if the black hole derives its ultimate mass  $M_\bullet$  from a halo of radius  $r_h$ , while  $r_s$  encloses the mass that forms the ultimate bulge mass  $M_s$  then

$$\frac{M_\bullet}{M_s} = \frac{r_h}{r_s}. \quad (35)$$

This assumes the pure inverse square density law, which might in fact have a logarithmic correction. In paper II, we shall find a slightly more general correlation that involves the self-similar memory. Taken at face value this simple relation gives  $r_h/r_s \approx 100$ .

## 7. Conclusions

We have attempted in this paper to find distribution functions that describe both dark matter bulges and a central black hole or at least a central mass concentration. Our method was to compare dynamically developing distribution functions to the results of simulations. These distribution functions develop nearly self-similarly and often retain an explicit memory of the self-similarity. The most successful DF is the FPDF which arises in the coarse graining expansion when all memory of the initial state is lost.

In the discussion of cusps and bulges, we were able to distinguish the Distribution function of Fridmann and Polyachenko (26) from that of Henriksen and Widrow (18). A shell code study confirmed the development of the latter modified by a cut-off. The FPDF was found to describe accurately the purely radial simulations of isolated collisionless halos carried out in (MacMillan 2006). These simulations retained cosmological initial conditions although non-radial forces were switched off. The final state is close to self-similar virialisation since the infall continues and memory of the initial state is lost. Moreover we show in the last section of the radial analysis that the FPDF appears in the self-similar coarse graining at zeroth order, if sensitivity to initial conditions is to be lost dynamically.

This correspondence between the theory and the simulations gives us some confidence in the DF's found by remaining 'close' to self-similarity. This is especially so since predictions describing the simulation results were based on  $a = 0.72$ , which was deduced elsewhere in the context of adiabatic self-similarity (H2007).

The FPDF may contain a central mass concentration that is unlikely to be a true black hole at least in the early stages. It may represent a central mass concentration or bulge initially. The growth time of such a central mass in a system of radial orbits is given simply by the dynamical time, so that this would be a rapid phase. Subsequently with the rise of dissipation and instabilities, there may be a slower phase of radial accretion towards the centre. It is possible that this cycle could repeat several times in a process we have referred to as 'interrupted accretion'. Under this process the  $r^{-2}$  density law would apply almost everywhere. The radial velocity dispersion is proportional to the potential. Thus it decreases as  $r^{-1}$  near the central mass, and subsequently decreases logarithmically with  $r$ .

The HWDF (18) is restricted to a strictly steady and self-similar bulge, but it has the merit of allowing a family of densities and potentials (velocity dispersion) according to the

self-similar prescription. A central mass is allowed only in the Keplerian limit wherein  $a = 3/2$ . This gives a massless bulge with  $\rho \propto r^{-3}$ . This is naturally iterated to give an inner flattening but continued iteration is effectively in powers of  $\ln r$ , which should therefore be small.

The HWDF gives a density that is linear in the potential and hence a self-consistent bulge is found from the Poisson equation. The density profile is never flatter than  $r^{-2.5}$  near the central mass and tends to  $r^{-3}$  in the near Keplerian limit of dominant central mass. This restricts the applicability to a region outside the central bulge (i.e. beyond the scale radius  $r_b$ ). It does not seem to be relevant to a near black hole domain.

Our final result concerning steady radial orbits concerned the special case  $a = 1$ . The DF is a Gaussian that has been found previously in coarse graining. We include it here as a second example of a radial DF that produces an  $r^{-2}$  density profile (Mutka 2009), although there is a logarithmic correction. It is not strictly self-similar.

In the next paper in this series (paper II), we shall extend the exploration of the cusps and DF to that produced by anisotropies in spherical symmetry.

## 8. Acknowledgements

RNH acknowledges the support of an operating grant from the canadian Natural Sciences and Research Council. The work of MLeD is supported by CSIC (Spain) under the contract JAEDoc072, with partial support from CICYT project FPA2006-05807, at the IFT, Universidad Autonoma de Madrid, Spain

## References

- Bahcall, J., & Wolf, R.A., 1976, ApJ, 209, 214.
- Bicknell, G.V. & Henriksen, R.N., ApJ, 232,670.
- Binney, J. & Tremaine, S., 1987. *Galactic Dynamics*, Princeton University Press, Princeton, New Jersey.
- Diemand, J., Kuhlen, M. & Madau, P., 2006, ApJ, 667,859.
- Ferrarese, L., & Merritt, D., 2000, ApJ, 539, L9.
- Fridman, A.M., & Polyachenko, V.L., 1984, *Physics of Gravitating Systems*, Springer, New York.
- Fujiwara, T., 1983, PASJ, 35, 547.
- Gebhardt, K., et al., 2000, ApJ, 539, L13.
- Gillessen, S., et al., 2009, ApJ, 692, 1075.
- Henriksen, R.N., Widrow, L.M., 1995, MNRAS, 276, 679.
- Henriksen, R.N., Widrow, L.M., 1999, MNRAS, 302, 321.
- Henriksen, R.N., & Le Delliou, M., 2002, MNRAS, 331, 423.
- Henriksen, R.N., 2006, MNRAS, 366, 697.
- Henriksen, R.N., 2006, ApJ, 653, 894.
- Henriksen, R.N., 2007, ApJ, 671, 1147.
- Henriksen, R.N., 2009, ApJ, 690, 102.
- Henriksen, R.N., Le Delliou, M., & MacMillan, J.D., 2009, subm. to A&A (I)
- Henriksen, R.N., Le Delliou, M., & MacMillan, J.D., 2009, subm. to A&A (II)
- Henriksen, R.N., Le Delliou, M., & MacMillan, J.D., 2009, subm. to A&A (III)
- Kurk, J.D., et al., 2007, ApJ, 669, 32.
- Kormendy, J., & Richstone, D., 1995, Ann.Rev.A&A.
- Kormendy, J., & Bender, R., 2009, ApJ, 691, L142.
- Le Delliou, M., 2001, PhD Thesis, Queen's University, Kingston, Canada.
- Lu, Yu, 2006, MNRAS, 368, 193.
- MacMillan, J.D., & Henriksen, R.N., 2002, ApJ, 569, 83.
- MacMillan, J.D., & Henriksen, R.N., 2003, Carnegie Observatories Astrophysics Series, 1, *Co-evolution of Black Holes and Galaxies*, L.C. Ho (ed.).
- MacMillan, J., 2006, PhD Thesis, Queen's University at Kingston, ONK7L 3N6, Canada.
- MacMillan, J.D., Widrow, L.M., & Henriksen, R.N., 2006, ApJ, 653, 43.
- Magorrian, J., et al., 1998, AJ, 115, 2285.
- Maiolino, R., et al., 2007, A&A, 472, L33.
- Merritt, D., & Szell, A., 2006, ApJ, 648, 890.
- Mutka, P., 2009, Proceeding of *Invisible Universe*, Palais de l'UNESCO, Paris, ed. J-M Alimi.
- Peirani, S. & de Freitas Pacheco, J.A., 2008, Phys. Rev. D, 77 (6), 064023.

- Nakano, T., Makino, M., 1999, *ApJ*, 525, L77.  
Navarro, J.F., Frenk, C.S., White, S.D.M., 1996, *ApJ*, 462, 5  
Peebles, P.J.E., 1972, *Gen.Rel.Grav.*, 3, 63.  
Quinlan, G.D., Hernquist, L., Sigurdsson, S., 1995, *ApJ*, 440, 554.  
van der Marel, R., 2009, in *Unveiling the Mass*, Queen's U., Kingston, Ontario,  
ed. S. Courteau.  
Young, P., 1980, *ApJ*, 242, 1232.  
Zhao, D.H. et al., 2003, *MNRAS*, 339, 12.  
Walter, F., et al., 2009, *Nature*, 457, 699.